

A Kinetic Study of the Oxidation of Water by Ce^{IV} Ions in Different Acid Media, Mediated by Thermally Activated Ruthenium Dioxide Hydrate

ANDREW MILLS* and SUSAN GIDDINGS

Department of Chemistry, University College of Swansea, Singleton Park, Swansea SA2 8PP, U.K.

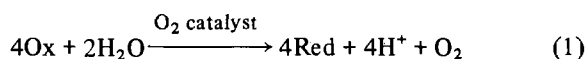
(Received August 5, 1988)

Abstract

A kinetic study was carried out of the oxidation of water to O₂ by Ce^{IV} ions in two different acid media, mediated by thermally activated ruthenium dioxide hydrate RuO₂·yH₂O*. The two different acid media were 0.5 mol dm⁻³ H₂SO₄ and 1 mol dm⁻³ HClO₄ + 3.5 × 10⁻² mol dm⁻³ H₂SO₄, respectively. In 0.5 mol dm⁻³ H₂SO₄ the kinetics were complicated by an inhibitive action exhibited by Ce^{III} ions. In 1 mol dm⁻³ HClO₄ + 3.5 × 10⁻² mol dm⁻³ H₂SO₄ the kinetics were much simpler, no inhibition by the Ce^{III} ions was observed and the kinetics were found to be first order with respect to [Ce⁴⁺] and [RuO₂·yH₂O*]. The results of the kinetic studies in the two different acid media were interpreted using an electrochemical model of the catalytic step, in which the particles of the RuO₂·yH₂O* powder dispersion act as microelectrodes through which electrons are transferred from the water to the Ce^{IV} ions.

Introduction

There are many oxidants which are thermodynamically capable of oxidising water to O₂ but few which can do so directly under ambient conditions, due to a high activation energy barrier. The oxidation of water to O₂ is an important reaction in a number of research areas including: industrial electrochemistry [1], green plant photosynthesis [2] and solar to chemical energy conversion [3]. It is hardly surprising, therefore, that there is a wide spread interest [3, 4] in new materials which are capable of mediating the oxidation of water to O₂ by strong oxidants, *i.e.*



where Ox could be Ce⁴⁺, MnO₄⁻ or BrO₃⁻, for

*Author to whom correspondence should be addressed.

example. However, it is surprising that although a few O₂ catalyst are known, little work has been carried out to find out how they work.

In a recent paper [5] we established that ruthenium dioxide hydrate (RuO₂·xH₂O) was a poor O₂ catalyst. Subsequent work showed [6] that RuO₂·xH₂O could be converted into an active, stable, efficient O₂ catalyst by annealing RuO₂·xH₂O at *ca.* 144 °C in air for 5 h. This new O₂ catalyst we have named thermally activated ruthenium dioxide hydrate, or RuO₂·yH₂O* for short. In this paper we describe the results of a rigorous kinetic study of the oxidation of water to O₂ by Ce^{IV} ions, mediated by RuO₂·yH₂O*, in two very different acid media. As we shall see the kinetics observed in the two acid media are quite different and the results of both kinetic studies lend support to an electrochemical model of O₂ catalysis by RuO₂·yH₂O*.

Experimental

Materials

The ruthenium dioxide hydrate was obtained from Johnson Matthey (Batch No. 061151) and converted to a good O₂ catalyst by annealing at 144 °C in air for 5 h. Previous work has established [6] that this process of thermal activation is effective for any sample of RuO₂·xH₂O, regardless of source. All Ce^{IV} solutions were made up from an analytical volumetric solution of 0.1 mol dm⁻³ Ce^{IV} sulphate solution in 1 mol dm⁻³ H₂SO₄. The 0.5 mol dm⁻³ H₂SO₄ and 1 mol dm⁻³ HClO₄ were prepared from their respective acids in concentrated form. Unless stated otherwise all chemicals were purchased from BDH and were of AnalaR grade. The water used was doubly distilled and deionised.

Preparation of a Stock Dispersion

In a kinetic study of this nature it is an essential prerequisite to be able to reproduce the dispersion consistently. This was achieved by using a stock dispersion of the catalyst, which was prepared using the following simple method. The thermally activated

ruthenium dioxide hydrate ($\text{RuO}_2 \cdot y\text{H}_2\text{O}^*$) was ground for 30 min in an agate ball mill. A 7 mg sample of this powder was placed in 100 cm^3 of a solution containing $0.5 \text{ mol dm}^{-3} \text{ H}_2\text{SO}_4$, or $1 \text{ mol dm}^{-3} \text{ HClO}_4$, depending upon the acid medium required. The dispersion was then subjected to ultrasound, from an ultrasound bath (Ultra Sonics Ltd., model 6442AE), for 10 min to provide a good dispersion. This dispersion was then stirred for 12 h and then left to settle. It was found that continued stirring of the dispersion led a gradual decrease in the average particle size, presumably due to grinding, and this in turn produced changes in the kinetics. The settled stock dispersion could be readily resuspended by shaking and, after stirring for a few minutes, used in a kinetic run to generate very reproducible decay traces. The stock dispersion was replaced every 7 days by a fresh stock dispersion.

Kinetic Studies

The rate of oxidation of water by Ce^{IV} ions mediated by $\text{RuO}_2 \cdot y\text{H}_2\text{O}^*$ was monitored via the rate of reduction of the Ce^{IV} ions. The decrease in Ce^{IV} ion concentration was monitored spectrophotometrically as a function of time, using a Perkin-Elmer Lambda 3 spectrophotometer. The wavelength at which this decay was monitored was determined by the initial concentration of Ce^{IV} ions. Thus, 430 nm was used over the range $3.5 \times 10^{-4} \text{ mol dm}^{-3} < [\text{Ce}^{4+}] \leq 3.5 \times 10^{-3} \text{ mol dm}^{-3}$ and 320 nm was used for $[\text{Ce}^{4+}]_s \leq 3.5 \times 10^{-4} \text{ mol dm}^{-3}$. The molar absorptivities of Ce^{IV} ions in $0.5 \text{ mol dm}^{-3} \text{ H}_2\text{SO}_4$ and $1 \text{ mol dm}^{-3} \text{ HClO}_4 + 3.5 \times 10^{-2} \text{ mol dm}^{-3} \text{ H}_2\text{SO}_4$ at 320 and 430 nm are given in Table 1.

TABLE 1. Molar Absorptivities of Ce^{IV} Ions in Different Acid Media

	$\epsilon(320 \text{ nm})$ ($\text{mol}^{-1} \text{ dm}^3 \text{ cm}^{-1}$)	$\epsilon(430 \text{ nm})$ ($\text{mol}^{-1} \text{ dm}^3 \text{ cm}^{-1}$)
$0.5 \text{ mol dm}^{-3} \text{ H}_2\text{SO}_4$	5580	290
$1 \text{ mol dm}^{-3} \text{ HClO}_4$ $+ 3.5 \times 10^{-2} \text{ mol dm}^{-3}$ H_2SO_4	4490	253

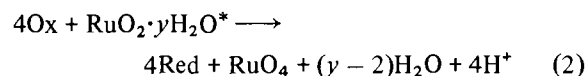
The first set of kinetic runs were carried out in a medium containing only $0.5 \text{ mol dm}^{-3} \text{ H}_2\text{SO}_4$. This was achieved by using a stock dispersion of $\text{RuO}_2 \cdot y\text{H}_2\text{O}^*$ (70 mg dm^{-3}) made up in $0.5 \text{ mol dm}^{-3} \text{ H}_2\text{SO}_4$, rather than $1 \text{ mol dm}^{-3} \text{ HClO}_4$. Another set of kinetic runs were carried out in an acidic medium which was $1 \text{ mol dm}^{-3} \text{ HClO}_4 + 3.5 \times 10^{-2} \text{ mol dm}^{-3} \text{ H}_2\text{SO}_4$, *i.e.* predominantly HClO_4 . In this work the H_2SO_4 was added either with the Ce^{IV} ions or prior to their injection. For example, in a typical kinetic run 90 mm^3 of a Ce^{IV} ion solution containing

$1 \text{ mol dm}^{-3} \text{ H}_2\text{SO}_4$ were injected into 2.5 cm^3 of the stock dispersion which was continually stirred at $1000 \text{ rev. min}^{-1}$. Within 3 s from the time of injection mixing of the two solutions was complete and the composition of the acidic medium was as required, *i.e.* $1 \text{ mol dm}^{-3} \text{ HClO}_4 + 3.5 \times 10^{-2} \text{ mol dm}^{-3} \text{ H}_2\text{SO}_4$. The time scale of the kinetics was always much greater than the mixing time. When injections of less than 90 mm^3 of a Ce^{IV} ion solution were made into the stock dispersion, the extra H_2SO_4 , necessary to produce a solution medium of $1 \text{ mol dm}^{-3} \text{ HClO}_4 + 3.5 \times 10^{-2} \text{ mol dm}^{-3} \text{ H}_2\text{SO}_4$ after mixing, was added to the dispersion prior to the injection.

After injection and mixing, the subsequent decay in the Ce^{IV} ion concentration was monitored spectrophotometrically and the data collected, stored and analysed on a microcomputer (Acorn model: BBC B).

The Flow System

A flow system was used to evaluate the ability of $\text{RuO}_2 \cdot y\text{H}_2\text{O}^*$ to act as an O_2 catalyst in either of the two acid media, *i.e.* $0.5 \text{ mol dm}^{-3} \text{ H}_2\text{SO}_4$ or $1 \text{ mol dm}^{-3} \text{ HClO}_4 + 3.5 \times 10^{-2} \text{ mol dm}^{-3} \text{ H}_2\text{SO}_4$. If $\text{RuO}_2 \cdot y\text{H}_2\text{O}^*$ is a good O_2 catalyst it should be able to catalyse reaction (1) efficiently without undergoing extensive anodic corrosion, *i.e.*



The flow system comprised a N_2 cylinder which provided a continuous flow of $180 \text{ cm}^3 \text{ min}^{-1}$ of gas through a series of 2 Dreschel bottles, each 125 cm^3 , and an oxygen membrane polarographic detector (O_2 -MPD). The first Dreschel bottle contained 100 cm^3 of a dispersion of 7 mg of $\text{RuO}_2 \cdot y\text{H}_2\text{O}^*$ in either $0.5 \text{ mol dm}^{-3} \text{ H}_2\text{SO}_4$ or $1 \text{ mol dm}^{-3} \text{ HClO}_4$. This Dreschel bottle had the additional feature of a rubber septum through which 3.6 cm^3 of a solution containing $0.1 \text{ mol dm}^{-3} \text{ Ce}^{\text{IV}}$ ions and $1 \text{ mol dm}^{-3} \text{ H}_2\text{SO}_4$ were injected. The second Dreschel bottle was a chemical trap for RuO_4 . In this trap were 100 cm^3 of a solution containing $0.1 \text{ mol dm}^{-3} \text{ NaOCl}$ in $1 \text{ mol dm}^{-3} \text{ NaOH}$. This solution was used to trap out, in the form of perruthenate ions [7], any RuO_4 produced in the reaction vessel and carried over by the N_2 stream. Any O_2 generated in the reaction vessel was detected quantitatively using the O_2 -MPD. A detailed description of the use of an O_2 -MPD for making such measurements in a flow system is given elsewhere [8].

The % corrosion undergone by the $\text{RuO}_2 \cdot y\text{H}_2\text{O}^*$ when used to catalyse the oxidation of water by Ce^{IV} ions in different acid media was calculated using the equation

$$\% \text{Corrosion} = \frac{[N(\text{RuO}_4^-)]}{[N(\text{RuO}_2 \cdot y\text{H}_2\text{O}^*)]} \times 100\% \quad (3)$$

where $N(\text{RuO}_4^-)$ is the number of moles of RuO_4^- collected in the RuO_4 trap (a quantity determined spectrophotometrically [9]) and $N(\text{RuO}_2 \cdot y\text{H}_2\text{O}^*)$ is the number of moles of $\text{RuO}_2 \cdot y\text{H}_2\text{O}^*$ in the reaction vessel, calculated via the measured % Ru content of the $\text{RuO}_2 \cdot y\text{H}_2\text{O}^*$ sample.

The % O_2 yield was calculated using the equation

$$\% \text{O}_2 \text{ yield} = N(\text{O}_2) \times 400 / N(\text{Ce}^{\text{IV}}) \quad (4)$$

where $N(\text{O}_2)$ is the number of moles of O_2 detected using the O_2 -MPD and $N(\text{Ce}^{\text{IV}})$ is the number of moles of Ce^{IV} ions injected into the reaction vessel (always 3.6×10^{-4} mol). The results of the work on the flow system are summarized in Table 2.

TABLE 2. % Corrosion and % O_2 Yields for $\text{RuO}_2 \cdot y\text{H}_2\text{O}^*$ in Different Acid Media

	O_2 yield (%)	Corrosion (%)
0.5 mol dm ⁻³ H_2SO_4	97	0
1 mol dm ⁻³ HClO_4 + 3.5×10^{-2} mol dm ⁻³ H_2SO_4	91	0

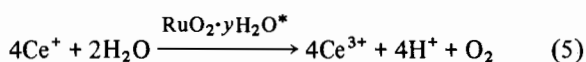
Other Methods

In all this work the gradient and intercept of a straight line plot were calculated using the method of least-squares and the errors quoted alongside the values are their respective standard deviations (σ).

Results

Ce^{IV} Reduction in H_2SO_4

From the results given in Table 2 it appears that in this system the reduction of Ce^{IV} ions is wholly associated with the oxidation of water to O_2 , *i.e.*



In a typical kinetic experiment 90 mm³ of a solution containing 0.1 mol dm⁻³ Ce^{IV} ions in 1 mol dm⁻³ H_2SO_4 were injected into 2.5 cm³ of a dispersion of $\text{RuO}_2 \cdot y\text{H}_2\text{O}^*$ (70 mg dm⁻³) in 0.5 mol dm⁻³ H_2SO_4 . The resulting absorbance *versus* time plot is illustrated in Fig. 1a. Unfortunately, in 0.5 mol dm⁻³ H_2SO_4 , the kinetics did not appear to be simple, thus a first order analysis of the data illustrated in Fig. 1a produced a curved rather than straight line, as illustrated in Fig. 1b.

A series of repeat injections of 20 mm³ of 0.1 mol dm⁻³ Ce^{IV} ions in 1 mol dm⁻³ H_2SO_4 was made into 2.5 cm³ of a $\text{RuO}_2 \cdot y\text{H}_2\text{O}^*$ dispersion (70 mg dm⁻³) in 0.5 mol dm⁻³ H_2SO_4 ; the $[\text{Ce}^{4+}]$ was allowed to decay to zero before each subsequent injection was made. The relative absorbance *versus* time plots for

the first five injections are illustrated in Fig. 2 by curves a–e. It is clear from these curves that the rate of reduction of the Ce^{IV} ions decreased as the number of injections made was increased. For example, the half life ($t_{1/2}$) for curve a was 35 s and this had increased to 162 s for curve e. The decay curve for the first injection gave a poor fit to both first and second law kinetics but with each subsequent injection the fit with second order kinetics improved. Other work has established [6] that the catalyst does not lose activity with repeated use. Decay curves identical to those illustrated in Fig. 2 by curves a–e were generated in a series of five experiments in which 20 mm³ of a solution containing 0.1 mol dm⁻³ Ce^{IV} ions in 1 mol dm⁻³ H_2SO_4 were injected into five lots of 2.5 cm³ of a $\text{RuO}_2 \cdot y\text{H}_2\text{O}^*$ dispersion (70 mg dm⁻³) in 0.5 mol dm⁻³ H_2SO_4 , to which had been added, respectively, 0, 20, 40, 60 and 80 mm³ of a solution containing 0.1 mol dm⁻³ Ce^{III} ions in 1 mol dm⁻³ H_2SO_4 . From these results it appears that Ce^{III} ions, generated by the reduction of Ce^{IV} ions via reaction (5), decrease the rate of reduction of the Ce^{IV} ions and are the cause for the broadening decay curves a–e, in Fig. 2.

It has been shown [10, 11] that a large number of redox catalysed reactions can be interpreted using an electrochemical model of the catalytic step. In this model it is assumed that the powdered catalyst acts as a polyelectrode and provides a medium through which electrons can be transferred from the water to the Ce^{IV} ions. Using this model it is possible to predict the kinetics of the redox catalysed reaction through a knowledge of the current–voltage curves on the redox catalyst of the two couples involved, in this case $\text{O}_2/\text{H}_2\text{O}$ and $\text{Ce}^{\text{IV}}/\text{Ce}^{\text{III}}$, and by assuming that at any time during the reaction the anodic current is numerically equal to the cathodic current. A detailed study of the kinetics of reaction (5) in 0.5 mol dm⁻³ H_2SO_4 has shown [12] that the observed kinetics for the reduction of the Ce^{IV} ions over a wide range of conditions can be interpreted successfully by assuming that the current–voltage curve for the $\text{O}_2/\text{H}_2\text{O}$ couple is that for a totally irreversible reaction and the current–voltage curve for the $\text{Ce}^{\text{IV}}/\text{Ce}^{\text{III}}$ couple is that for a totally reversible (Nernstian) reaction.

Using this model it can be shown [12, 13] that the Ce^{III} ions will reduce the rate of reduction of the Ce^{IV} ions and cause the type of decay curves illustrated in Fig. 2, assuming the equilibrium potentials for the two current–voltage curves are not very well separated. This situation is illustrated in Fig. 3 by the current–voltage curve for the irreversible oxidation of water, curve a, and the current–voltage curve for the reversible reduction of Ce^{IV} ions when the $[\text{Ce}^{\text{IV}}]/[\text{Ce}^{\text{III}}]$ ratio is b, 9:1; c, 1:1; and d, 1:9; respectively. In theory, with the first injection, *i.e.* curve a Fig. 2, the $\text{Ce}^{\text{IV}}/\text{Ce}^{\text{III}}$ ratio changes from

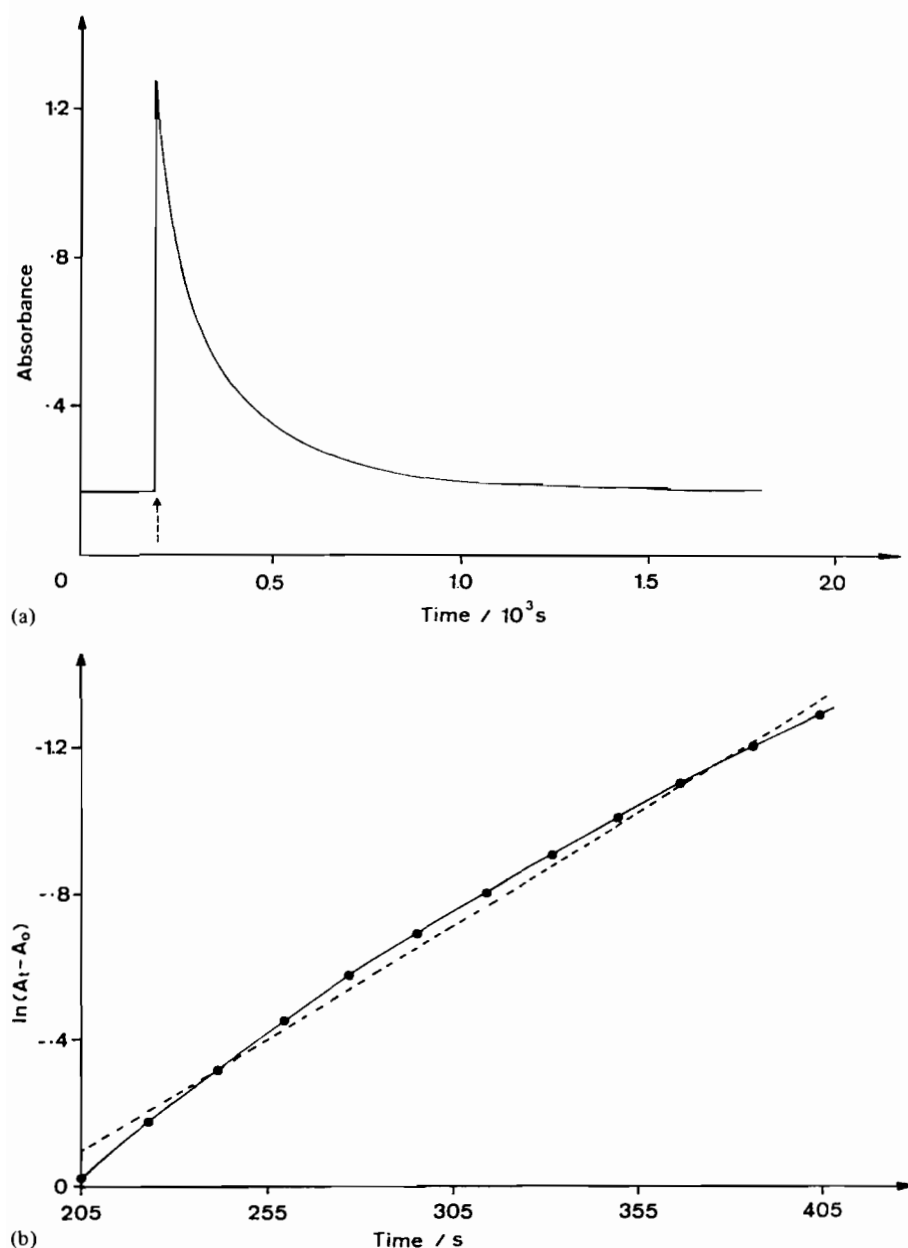


Fig. 1. (a) Absorbance-time profile recorded at 430 nm for the injection and subsequent decay of a solution containing Ce^{IV} ions (90 mm^3 of $0.1 \text{ mol dm}^{-3} \text{ Ce}^{\text{IV}}$ ions in $1 \text{ mol dm}^{-3} \text{ H}_2\text{SO}_4$) in a $\text{RuO}_2 \cdot y\text{H}_2\text{O}^*$ dispersion (2.5 cm^3 , 70 mg dm^{-3}) in $0.5 \text{ mol dm}^{-3} \text{ H}_2\text{SO}_4$. The broken vertical arrow denotes the point of injection. (b) Solid line: first order plot of the data illustrated in (a) where A_t is the absorbance at time t after the injection was made and A_0 is the absorbance just before the injection was made. Broken line: line of best fit to the data, calculated from a least-squares analysis of the data.

$\infty:1$ to $1:\infty$ as the $[\text{Ce}^{4+}]$ decays to zero. Thus curves b, c and d in Fig. 3 can be considered to represent the current-voltage curves for the $\text{Ce}^{\text{IV}}/\text{Ce}^{\text{III}}$ couple after 10%, 50% and 90% of the Ce^{IV} ions first injected have been reduced. The broken vertical lines in Fig. 3 identify the mixture potential on the redox catalyst (E_{mix}) and the mixture current, i_{mix} , at the three different stages of the reduction of Ce^{IV} ions, for the first injection.

From the broken vertical line connecting curves a and b in Fig. 3 it is clear that at in the initial part of the reaction, *i.e.* the first 10% at least, the rate of reduction of Ce^{IV} ions is near to diffusion controlled since i_{mix} lies close to the plateau region of curve b. However, near to the end of the reaction, *i.e.* the last 10% say, illustrated by curves a and c, the mixture current is further away from the plateau region of curve c and so i_{mix} and, therefore, the rate is signifi-

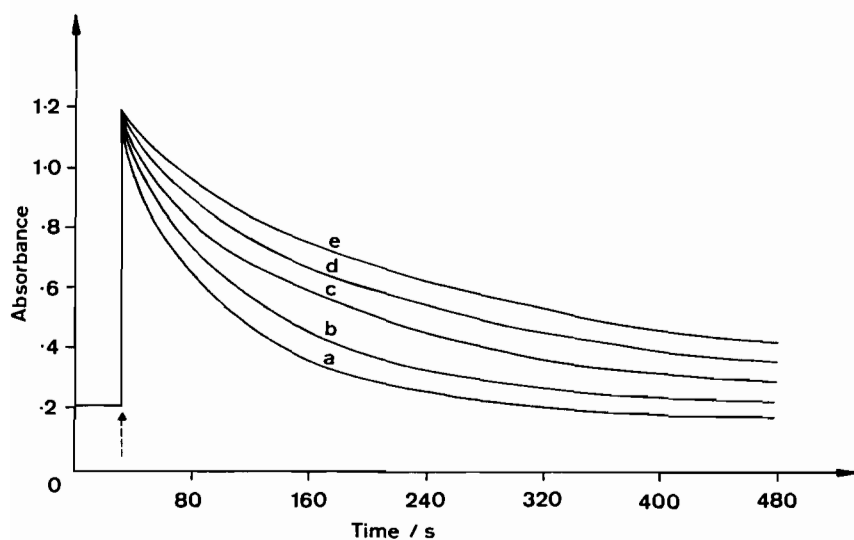


Fig. 2. Relative absorbance–time plots recorded at 430 nm for a series of repeat injections of 20 mm³ of a solution containing 0.1 mol dm⁻³ Ce^{IV} ions in 1 mol dm⁻³ H₂SO₄. The injections were made into the same dispersion of RuO₂·yH₂O* (2.5 cm³, 70 mg dm⁻³). The decay curves a–e are for the first to the fifth injection of Ce^{IV} ions. A relative absorbance change of 1.0 corresponds to an observed absorbance change of 0.264.

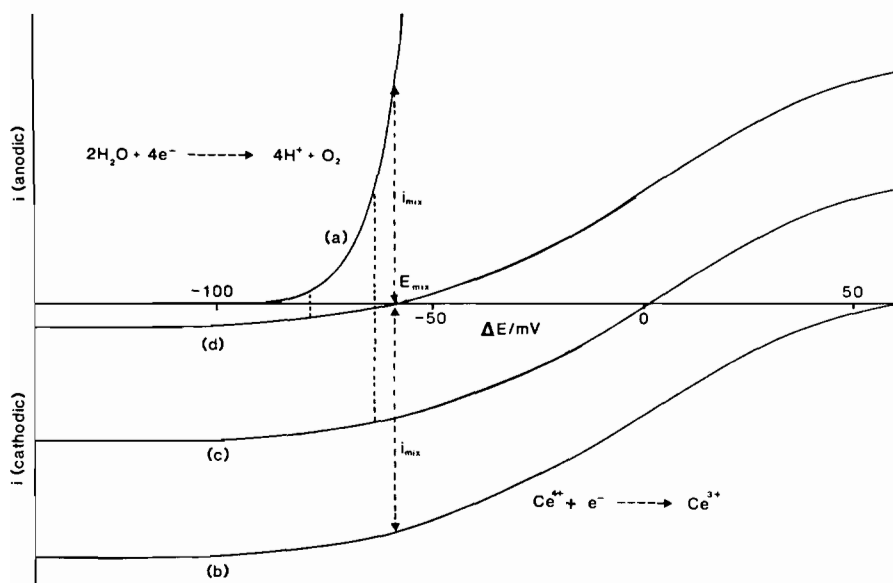


Fig. 3. Current–voltage curves for the O₂/H₂O couple (curve a) and the Ce^{IV}/[Ce^{III}] couple where the [Ce⁴⁺]/[Ce^{III}] ratio is: 9:1 (curve b), 1:1 (curve c) and 1:9 (curve d). These curves were generated using equations which assumed that the oxidation of water was an irreversible process and the reduction of Ce^{IV} ions was a nernstain process [12, 13]. In this Figure the equilibrium potentials of the two couples are not very well separated and as a result the mixture current is less than diffusion controlled. The broken vertical lines identify the mixture potential and the mixture current, *i.e.* when the anodic current, due to the oxidation of water, is equal to the cathodic current, due to the reduction of Ce^{IV} ions.

cantly less than diffusion controlled. Thus, when the current–voltage curves for the two couples are poorly separated, as illustrated in Fig. 3, the rate of reduction of Ce^{IV} ions will appear to slow down as the reaction proceeds due to the accumulation of Ce^{III} ions. These qualitative predictions are in agreement with the observed kinetics illustrated in Figs. 1a

and 2. However, the electrochemical model and associated equations used to generate the curves illustrated in Fig. 3 also suggest that for the first injection, when the [Ce³⁺] is low, the initial rate of reduction of Ce^{IV} ions will be approximately diffusion controlled and, therefore, will depend directly upon [Ce⁴⁺] and [RuO₂·yH₂O*], *vide infra*. A

kinetic study was carried out in which the initial rate of reduction of Ce^{IV} ions was measured as a function of $[\text{Ce}^{4+}]$, over the range $(3.5\text{--}0.4) \times 10^{-3} \text{ mol dm}^{-3}$ and as a function of $[\text{RuO}_2 \cdot \gamma\text{H}_2\text{O}^*]$, over the range $200\text{--}2 \text{ mg dm}^{-3}$. From the results of this work the initial rate of reaction did, indeed, appear to be first order with respect to both $[\text{Ce}^{4+}]$ and $[\text{RuO}_2 \cdot \gamma\text{H}_2\text{O}^*]$, as predicted by the electrochemical model.

Ce^{IV} Reduction in HClO_4 + some H_2SO_4

A prediction of the electrochemical model is that if the current–voltage curves for the $\text{O}_2/\text{H}_2\text{O}$ and $\text{Ce}^{\text{IV}}/\text{Ce}^{\text{III}}$ couples are very well separated then the mixture current should always lie in the plateau region of the $\text{Ce}^{\text{IV}}/\text{Ce}^{\text{III}}$ current–voltage curve [13]. Under these conditions the mixture current, and therefore the rate of reduction of Ce^{IV} ions, would be purely diffusion controlled, *i.e.*

$$i_{\text{mix}} = nFD[\text{Ce}^{4+}]A/\delta \quad (6)$$

where n is the number of electrons transferred in the reduction of Ce^{IV} to Ce^{III} , D is the diffusion coefficient for the Ce^{IV} species in the acid medium under examination, A is the surface area available for catalysis and is directly proportional to $[\text{RuO}_2 \cdot \gamma\text{H}_2\text{O}^*]$, and δ is the thickness of the diffusion layer. δ is essentially a function of the hydrodynamic flow conditions around the microelectrode particles; in our experiments these conditions were fixed by using a constant stirring rate in all kinetic runs. Under these conditions the electrochemical model predicts via eqn. (6) that the rate of reduction of Ce^{IV} ions will be diffusion controlled and depend directly upon $[\text{Ce}^{4+}]$ and $[\text{RuO}_2 \cdot \gamma\text{H}_2\text{O}^*]$, but independent of $[\text{Ce}^{3+}]$.

These predictions and the validity of the electrochemical model can be tested, since the current–voltage curve for the $\text{Ce}^{\text{IV}}/\text{Ce}^{\text{III}}$ couple can be shifted to more positive potentials by changing the acid medium [11]. In $0.5 \text{ mol dm}^{-3} \text{ H}_2\text{SO}_4$ the Ce^{IV} and Ce^{III} ions are complexed with sulphate ions whereas in $1 \text{ mol dm}^{-3} \text{ HClO}_4$ the Ce^{IV} and Ce^{III} ions are largely uncomplexed [14, 15]. As a result the formal redox potential of the $\text{Ce}^{\text{IV}}/\text{Ce}^{\text{III}}$ couple ($E^{\text{or}}(\text{Ce}^{\text{IV}}/\text{Ce}^{\text{III}})$) in $0.5 \text{ mol dm}^{-3} \text{ H}_2\text{SO}_4$ is 1.44 V *versus* NHE and is significantly lower than $E^{\text{or}}(\text{Ce}^{\text{IV}}/\text{Ce}^{\text{III}})$ in $1 \text{ mol dm}^{-3} \text{ HClO}_4$, which is 1.70 V *versus* NHE [14]. In order to carry out reaction (5) in an acidic medium containing HClO_4 and no H_2SO_4 it would be necessary to prepare Ce^{IV} perchlorate. Unfortunately, the preparation of this compound is both a lengthy and involved process [15], thus, for practical purposes, it was decided to carry out a kinetic study of reaction (5), using an acid medium which was predominantly HClO_4 , *i.e.* $1 \text{ mol dm}^{-3} \text{ HClO}_4 + 3.5 \times 10^{-2} \text{ mol dm}^{-3} \text{ H}_2\text{SO}_4$. In this medium the formal potential of the $\text{Ce}^{\text{IV}}/\text{Ce}^{\text{III}}$ couple was measured as 1.58 V

versus NHE, *i.e.* 140 mV more positive than that in $0.5 \text{ mol dm}^{-3} \text{ H}_2\text{SO}_4$.

From the results given in Table 2 it would appear that the reduction of Ce^{IV} ions in $1 \text{ mol dm}^{-3} \text{ HClO}_4 + 3.5 \times 10^{-2} \text{ mol dm}^{-3} \text{ H}_2\text{SO}_4$, mediated by $\text{RuO}_2 \cdot \gamma\text{H}_2\text{O}^*$, occurs with the concomitant oxidation of water to O_2 . Thus, the overall reaction may be expressed by eqn. (5). In a typical kinetic experiment 90 mm^3 of a solution containing $0.1 \text{ mol dm}^{-3} \text{ Ce}^{\text{IV}}$ ions in $1 \text{ mol dm}^{-3} \text{ H}_2\text{SO}_4$ were injected into 2.5 cm^3 of the stock dispersion of $\text{RuO}_2 \cdot \gamma\text{H}_2\text{O}^*$ in $1 \text{ mol dm}^{-3} \text{ HClO}_4$. The recorded absorbance *versus* time plot is illustrated in Fig. 4a. A first order plot over three half lives of the data illustrated in Fig. 4a is given in Fig. 4b. This plot is a perfect straight line (correlation coefficient (r) = 1.0000) with a gradient = $-3.8 \times 10^{-2} \text{ s}^{-1}$. In a series of experiments the amount of Ce^{IV} ions injected was varied so as to produce, after mixing, a variety of initial concentrations of Ce^{IV} ions over the range 3.5×10^{-3} to $3.9 \times 10^{-5} \text{ mol dm}^{-3}$. In each case a first order plot of the decay data gave an excellent straight line ($r = \geq 0.9999$). The average value for the first order decay constant ($k_1 = -m$) was found to be $4.8 \times 10^{-2} \text{ s}^{-1}$. These results appear to confirm that the prediction of the electrochemical model that the rate of reduction of Ce^{IV} ions in $1 \text{ mol dm}^{-3} \text{ HClO}_4 + 3.5 \times 10^{-2} \text{ mol dm}^{-3} \text{ H}_2\text{SO}_4$, via reaction (5), is first order with respect to the $[\text{Ce}^{4+}]$.

A series of repeat injections of 20 mm^3 of a solution containing $0.1 \text{ mol dm}^{-3} \text{ Ce}^{\text{IV}}$ ions and $1 \text{ mol dm}^{-3} \text{ H}_2\text{SO}_4$ were made into 2.5 cm^3 of the stock dispersion of $\text{RuO}_2 \cdot \gamma\text{H}_2\text{O}^*$; the $[\text{Ce}^{4+}]$ was allowed to fall to zero before each new injection was made. Unlike a similar experiment carried out in $0.5 \text{ mol dm}^{-3} \text{ H}_2\text{SO}_4$ and reported above (see Fig. 2), each of the decay traces were identical and had a half life of 21 s . From this work it appears that the rate of reduction of Ce^{IV} ions in $1 \text{ mol dm}^{-3} \text{ HClO}_4 + 3.5 \times 10^{-2} \text{ mol dm}^{-3} \text{ H}_2\text{SO}_4$ is independent of the concentration of Ce^{III} ions present, once again confirming the prediction made by the electrochemical model.

In a separate set of experiments the value of k_1 was measured as a function of $[\text{RuO}_2 \cdot \gamma\text{H}_2\text{O}^*]$ over the range $12\text{--}140 \text{ mg dm}^{-3}$, using a fixed initial concentration of Ce^{IV} ions of $3.5 \times 10^{-4} \text{ mol dm}^{-3}$. A plot of $\ln(k_1)$ *versus* $\ln[\text{RuO}_2 \cdot \gamma\text{H}_2\text{O}^*]$ yielded a good straight line ($r = 0.9901$). A least-squares analysis of the data showed the following: number of points (n) = 8, gradient (m) = 1.04 ± 0.06 and intercept (c) = -7.99 ± 0.25 . From this work it appears that the rate of reduction of Ce^{IV} ions in $1 \text{ mol dm}^{-3} \text{ HClO}_4 + 3.5 \times 10^{-2} \text{ mol dm}^{-3} \text{ H}_2\text{SO}_4$ depends directly upon the concentration of the redox catalyst present. These findings lend further support to the electrochemical model used to interpret the kinetics.

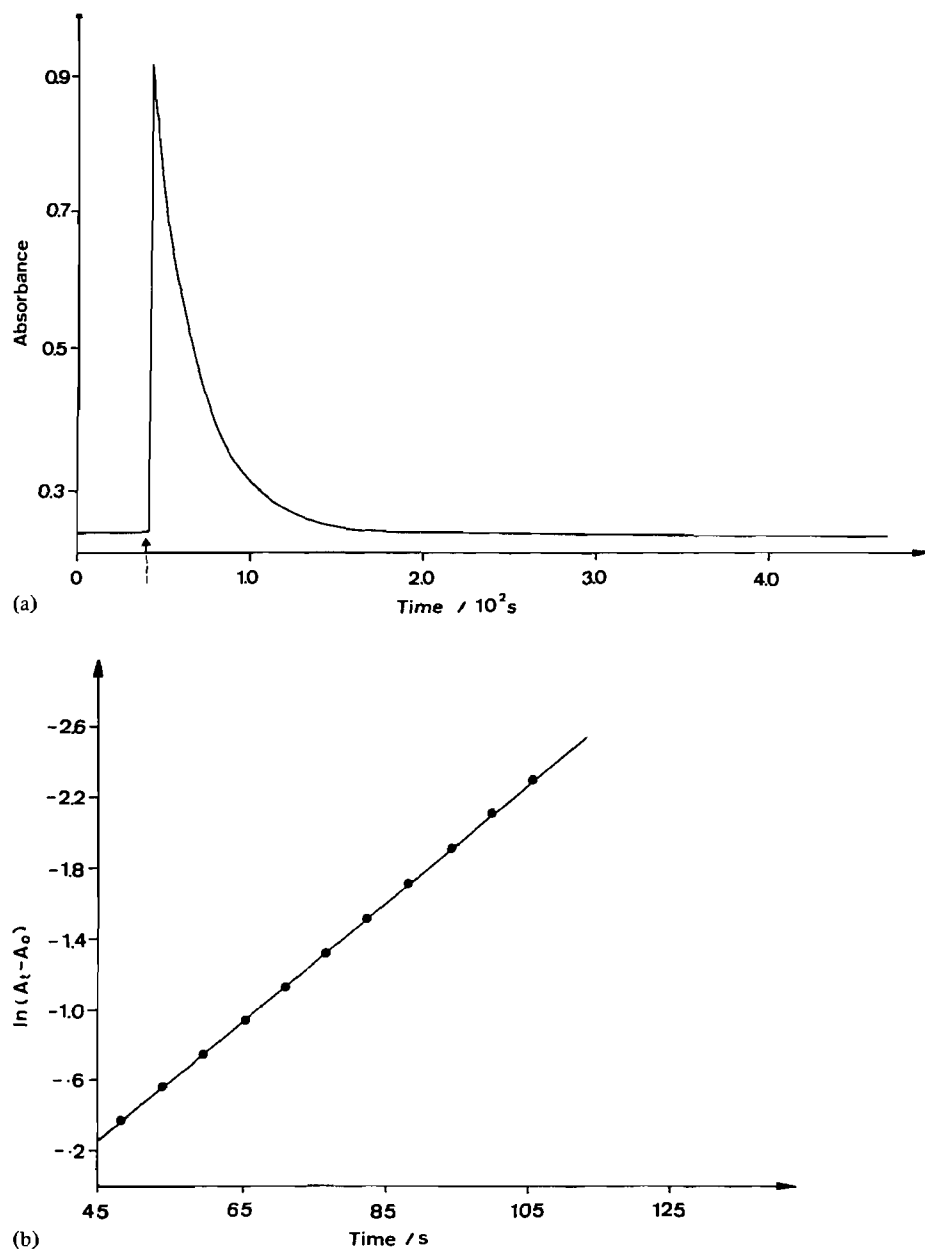


Fig. 4. (a) Absorbance–time profile recorded at 430 nm for the injection and subsequent decay of a solution containing Ce^{IV} ions (90 mm^3 of $0.1 \text{ mol dm}^{-3} Ce^{IV}$ ions in $1 \text{ mol dm}^{-3} H_2SO_4$) into a $RuO_2 \cdot \gamma H_2O^*$ dispersion (2.5 cm^3 , 70 mg dm^{-3}) in $1 \text{ mol dm}^{-3} H_2SO_4 HClO_4$. The broken vertical arrow denotes the point of injection. (b) First order plot of the data illustrated in (a), where A_t is the absorbance at time t after the injection was made and A_0 is the absorbance just before the injection was made.

In a final set of experiments the variation in k_1 was measured as a function of temperature using a fixed concentration of catalyst (70 mg dm^{-3}) and a fixed concentration of Ce^{IV} ions ($3.5 \times 10^{-4} \text{ mol dm}^{-3}$). The subsequent Arrhenius-type plot of $\ln(k_1)$ versus T^{-1} is illustrated in Fig. 5. A least-squares analysis of the data shown in Fig. 5 yielded the following information: $n = 6$, $m = -2610 \pm 250 \text{ K}$, $c = 5.36 \pm 0.78$ and $r = 0.9901$. The activation

energy for the catalysed reaction (5) was calculated from the value of the gradient to be $22 \pm 2 \text{ kJ mol}^{-1}$. The electrochemical model predicts that the activation energy for reaction (5), in $1 \text{ mol dm}^{-3} HClO_4 + 3.5 \times 10^{-2} \text{ mol dm}^{-3} H_2SO_4$, should be that for a diffusion controlled reaction, *i.e.* typically 15 kJ mol^{-1} [16]. The experimentally determined value of 22 kJ mol^{-1} is, therefore, in quite good agreement with that predicted by the electrochemical model.

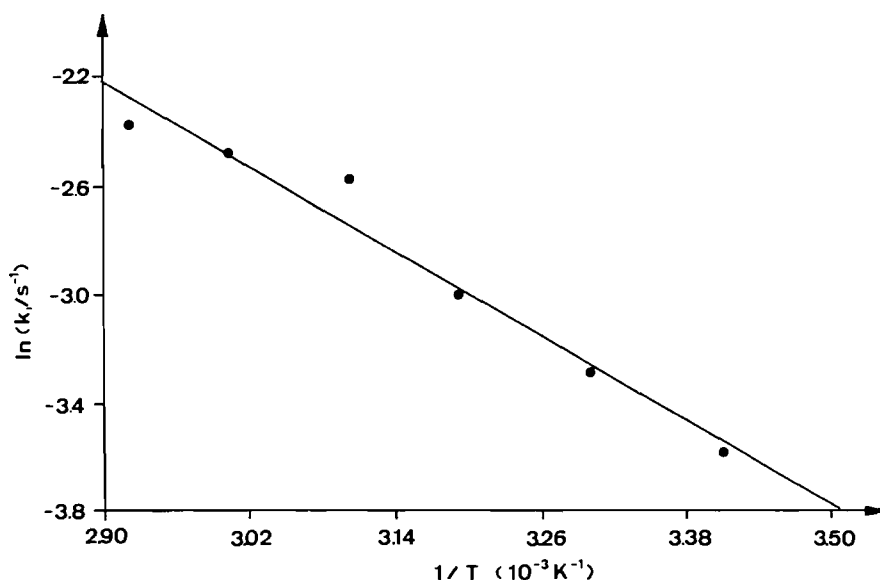


Fig. 5. Arrhenius-type plot of k_1 vs. T^{-1} . The temperature range studied was from 20 to 50 °C.

Conclusions

$\text{RuO}_2 \cdot y\text{H}_2\text{O}^*$ is able to mediate the oxidation of water to O_2 by Ce^{IV} ions in both $0.5 \text{ mol dm}^{-3} \text{ H}_2\text{SO}_4$ and $1 \text{ mol dm}^{-3} \text{ HClO}_4 + 3.5 \times 10^{-2} \text{ mol dm}^{-3} \text{ H}_2\text{SO}_4$. In the former acid medium, the rate of reduction of the Ce^{IV} ions decreases as the concentration of Ce^{III} ions increases. These results can be interpreted using an electrochemical model of the redox catalysed reaction. In this model the $\text{RuO}_2 \cdot y\text{H}_2\text{O}^*$ powder acts as a polyelectrode, providing a medium for electrons to be transferred from the water, via an irreversible reaction, to the Ce^{IV} ions, via a highly reversible reaction. Although Ce^{III} ions complicate the kinetics, in the initial part of the reaction, when the concentration of Ce^{III} ions is low, the rate of reduction of Ce^{IV} ions should, according to the electrochemical model, be approximately diffusion controlled and, therefore, first order with respect to $[\text{Ce}^{4+}]$ and $[\text{RuO}_2 \cdot y\text{H}_2\text{O}^*]$. These predictions were confirmed in an initial rate study. It can be argued, using the electrochemical model, that in an acid medium consisting of mainly HClO_4 , i.e. $1 \text{ mol dm}^{-3} \text{ HClO}_4 + 3.5 \times 10^{-2} \text{ mol dm}^{-3} \text{ H}_2\text{SO}_4$, the rate of reduction of Ce^{IV} ions should be first order with respect to $[\text{Ce}^{4+}]$ and $[\text{RuO}_2 \cdot y\text{H}_2\text{O}^*]$, but independent of the $[\text{Ce}^{3+}]$. These predictions were once again confirmed by experiment. Further support for the electrochemical model was provided by the experimentally determined value for the activation energy for the reaction which was close to that expected for a diffusion controlled reaction. The findings reported in this paper provide

very strong evidence that the O_2 catalyst, $\text{RuO}_2 \cdot y\text{H}_2\text{O}^*$, works as a polyelectrode when catalysing the oxidation of water by strong oxidants, such as Ce^{IV} ions. Although this model has often been assumed [3, 17] in O_2 catalysis, there have been few [10] attempts to test it. This work represents an important step forward in our understanding of heterogeneous O_2 catalysis.

Acknowledgement

We thank the SERC for supporting this work.

References

- 1 S. Trasatti and G. Lodi, in S. Trasatti (ed.), *Electrodes of Conductive Metallic Oxides*, Part B, Elsevier, Amsterdam, 1980.
- 2 A. Harriman and J. Barber, in J. Barber (ed.), *Topics of Photosynthesis*, Elsevier, Amsterdam, 1979.
- 3 M. Grätzel (ed.), *Energy Resources through Photochemistry and Catalysis*, Academic Press, New York, 1983.
- 4 D. Pletcher, *J. Appl. Electrochem.*, **14** (1984) 403.
- 5 A. Mills, S. Giddings and I. Patel, *J. Chem. Soc., Faraday Trans. 1*, **83** (1987) 2317.
- 6 A. Mills, S. Giddings, I. Patel and C. Lawrence, *J. Chem. Soc., Faraday Trans. 1*, **83** (1987) 2331.
- 7 R. P. Larson and L. E. Ross, *Anal. Chem.*, **31** (1959) 176.
- 8 A. Mills and C. Lawrence, *Analyst (London)*, **109** (1984) 1549.
- 9 J. L. Woodhead and J. M. Fletcher, *J. Chem. Soc.*, (1961) 5039.

- 10 M. Spiro and A. B. Ravnö, *J. Chem. Soc.*, (1965) 78.
- 11 M. Spiro, *Chem. Soc. Rev.*, 15 (1986) 141.
- 12 A. Mills and N. McMurray, *J. Chem. Soc., Faraday Trans. I*, accepted for publication (MS no. 8/02863J/FIP).
- 13 A. Mills and N. McMurray, *J. Chem. Soc., Faraday Trans., I*, accepted for publication (MS no. 8/02863H/FIP).
- 14 G. F. Smith and Ca. A. Getz, *Ind. Eng. Chem., Anal. Ed.*, 10 (1938) 191.
- 15 R. L. Moore and R. C. Anderson, *J. Am. Soc.*, 67 (1945) 167.
- 16 F. Wilkinson, *Chemical Kinetics and Reaction Mechanisms*, Van Nostrand Reinhold, London, 1981, p. 140.
- 17 K. Kalyanasundaram, O. Micic, E. Pramauro and M. Grätzel, *Helv. Chim. Acta*, 62 (1979) 2432.